42. Y. Amelin, E. Y. Ritsk, L. A. Neymark, *Earth Planet. Sci. Lett.* **148**, 299 (1997).
43. Individual chondrules were extracted from the Acfer 059 meteorite by using stainless-steel tools. Fractions consisting of chondrule fragments of uniform appearance were picked from a coarsely crushed portion of the meteorite. Chondrules and fragments were first cleaned by ultrasonic agitation in ethanol to remove adhering matrix minerals, weighed, and crushed to about <50 μm pieces with an aluminum oxide mortar and pestle. Preparation of the CAI fractions was similar, but the starting CAI fragments were coarsely crushed instead of pulverizing. Final cleaning was performed by five or six 10-min cycles of ultrasonic agitation in 0.5 to 2.0 M high-purity HCl in Savillex vials, which were subsequently used for digestion. During early analyses (chondrules 1 to 5), acid leachates from several fractions were preserved and analyzed separately. One chondrule and matrix sample were analyzed without acid leaching. During the later stages, chondrules were subjected to a more intensive acid leaching before crushing: three to five 30-min cycles of ultrasonic agitation in ethanol plus 6 M HCl 1:1 mixture. This treatment effectively removed all residual matrix from the surface of chondrules and helped to minimize the common Pb content, but it also caused etching and, in some cases, bleaching of chondrules and chondrule fragments. In addition, this treatment partially removed chondrule rims.
44. Y. Amelin, *Lunar Planet Sci.* **32**, 1389 (2001).
45. E. Rotenberg, Y. Amelin, *Eleventh Annual V.M. Goldschmidt Conference*, Hot Springs, VA, 20 to 24 May 2001, no. 3626.
46. Y. Amelin, in preparation.
47. J. W. Arden, G. Cressey, *Geochim. Cosmochim. Acta* **48**, 1899 (1984).
48. Primordial Pb is the Pb present in the solar system at the time of its formation. This is the least radiogenic Pb known, which is preserved, nearly unchanged, in the mineral troilite (FeS) in some iron meteorites (*58*, *59*). Modern common Pb is a mixture of primordial Pb and 20 to 50% additions of radiogenic ^{206}Pb, ^{207}Pb, and ^{208}Pb accumulated since formation of the Earth and meteorite parent bodies.
49. F. Tera, R. W. Carlson, *Geochim. Cosmochim. Acta* **63**, 1877 (1999).
50. "Errorchron" is a term for an isochron with the scatter of the data exceeding analytical uncertainties. The excess scatter implies that the conditions of isochron model were not precisely fulfilled, e.g., the samples are not coeval, or the common Pb isotopic composition is variable, or the U-Pb systems of the samples were disturbed in the past. Thus, the errorchron dates may be inaccurate and should be interpreted with caution.
51. Y. Amelin *et al.*, *Lunar Planet Sci.* **33**, 1151 (2002).
52. J. H. Chen, G. J. Wasserburg, *Earth Planet. Sci. Lett.* **52**, 1 (1981).
53. Mg isotope compositions were measured with PANURGE, a modified Cameca IMS-3f ion microprobe, at Lawrence Livermore National Laboratory, with the operating conditions and procedures as described (*60*). The Mg isotope ratios were corrected for both instrumental and intrinsic fractionation, assuming the standard ratios of $^{25}Mg/^{24}Mg = 0.12663$ and $^{26}Mg/^{24}Mg = 0.13932$ (*61*). The corrected ratios $(^{26}Mg/^{24}Mg)_C$ were used to calculate $\delta^{26}Mg = [(^{26}Mg/^{24}Mg)_C/0.13932 - 1] \times 1000$.
54. D. J. Cherniak, *Chem. Geol.* **177**, 381 (2001).
55. The error of 1.2 My in the CAI to chondrule formation interval (a simple sum of individual errors) is the most conservative estimate, which corresponds to the case of anticorrelated errors. A more probable estimate, for the case of uncorrelated errors, is 0.9 My (a quadratic sum of individual errors).
56. A. P. Boss, *Lunar Planet. Sci.* **31**, 1084 (2000).
57. G. Faure, *Principles of Isotope Geology* (Wiley, New York, 1986).
58. M. Tatsumoto, R. J. Knight, C. J. Allégre, *Science* **180**, 1279 (1973).
59. C. Göpel, G. Manhés, C. J. Allégre, *Geochim. Cosmochim. Acta* **49**, 1681 (1985).
60. I. D. Hutcheon, J. A. Armstrong, G. J. Wasserburg, *Geochim. Cosmochim. Acta* **51**, 3175 (1987).
61. E. J. Catanzaro, T. J. Murphy, E. L. Garner, W. R. Shields, *J. Res. Natl. Bur. Stand.* **70A**, 453 (1966).
62. We are grateful to A. Greshake for providing samples of Acfer 059. This work was supported by Canadian Space Agency contract 9F007-010128/001/SR (Y.A., principal investigator) and NASA grants NAG5-10610 (A.N.K., principal investigator) and NAG5-11591 (K. Keil, principal investigator). Work performed under the auspices of the U.S. Department of Energy by Lawrence Livermore National Laboratory under contract W-7405-ENG-48.

Supporting Online Material
www.sciencemag.org/cgi/content/full/297/5587/1678/DC1
Table S1

14 May 2002; accepted 29 July 2002

Diamond Genesis, Seismic Structure, and Evolution of the Kaapvaal-Zimbabwe Craton

Steven B. Shirey,[1*] Jeffrey W. Harris,[2] Stephen H. Richardson,[3] Matthew J. Fouch,[4] David E. James,[1] Pierre Cartigny,[5] Peter Deines,[6] Fanus Viljoen[7]

The lithospheric mantle beneath the Kaapvaal-Zimbabwe craton of southern Africa shows variations in seismic P-wave velocity at depths within the diamond stability field that correlate with differences in the composition of diamonds and their syngenetic inclusions. Middle Archean mantle depletion events initiated craton keel formation and early harzburgitic diamond formation. Late Archean accretionary events involving an oceanic lithosphere component stabilized the craton and contributed a younger Archean generation of eclogitic diamonds. Subsequent Proterozoic tectonic and magmatic events altered the composition of the continental lithosphere and added new lherzolitic and eclogitic diamonds to the Archean diamond suite.

Seismic imaging of the lithospheric mantle beneath the Kaapvaal-Zimbabwe cratons and the Limpopo mobile belt (*1–4*) has produced a detailed picture of the source region for diamonds (Fig. 1). We place two decades of study of some 4000 diamonds from southern Africa's major diamond deposits (*5*, *6*) into geologic context at lithospheric source depths to relate diamond formation to the processes of craton creation, assembly, and modification. Diamond formation worldwide is associated with the presence of ancient lithospheric mantle keels beneath cratons (*7*, *8*). In the Archean keel of the Kaapvaal-Zimbabwe craton, mantle peridotite and eclogite host multiple generations of both Archean and Proterozoic (*9*) diamonds (*6*, *10*, *11*) that have been sampled by later kim-

Table 1. Seismic velocity of the lithospheric mantle, diamond composition ($\delta^{13}C$, N, and type Ia), and inclusion paragenesis for southern African diamonds. Seismic velocities are for P-waves (in % deviation from a cratonic reference model) through a 50-km-radius cylinder of mantle extending from 150 km to 225 km depth below the major diamond mines (*2*, *3*). Studies of C isotopes and N have been carried out on more than 900 individual diamonds enclosing silicate, oxide, and sulfide inclusions. Parageneses (P, peridotitic; E, eclogitic; W, websteritic) are listed in order of abundance; subordinate parageneses are in parentheses. Nitrogen concentration is the average of the total diamond population as measured by Fourier transform infrared spectroscopy (FTIR); De Beers Pool data is measured by mass spectrometry. Type Ia data are the % of diamonds in the studied population with aggregated nitrogen >20 ppm. Sources of data are as follows: De Beers Pool (*22*, *23*), Finsch (*25*, *29*), Jagersfontein (*28*), Jwaneng (*23*), Koffiefontein (*28*), Letlhakane (*51*), Orapa (*24*, *52*), Premier (*25*, *29*, *53*), Roberts Victor (*27*), and Venetia (*54*).

Location	Seismic velocity	$\delta^{13}C$ (‰)	N (ppm)	Type Ia (%)	Paragenesis
Jwaneng	−0.006	−19 to −2	400	91	E,P
Letlhakane	−0.008		345	87	E,P
Orapa	−0.010	−26 to −3	478	94	E,P,(W)
Premier	−0.209	−14 to −2	413	90	E,P
Venetia	0.194	−18 to −2	259	77	P,(E,W)
De Beers Pool	0.245	−16 to −1	170	55	P,(E)
Finsch	0.084	−8 to −3	199	74	P,(E)
Roberts Victor	0.211	−16 to −3	260	73	P,(E)
Jagersfontein	0.357	−21 to −3	291	81	E,P
Koffiefontein	0.327	−17 to −2	201	85	P,E

Science

6 September 2002

Vol. 297 No. 5587
Pages 1597–1756 $9

American Association for the Advancement of Science

berlites [65 to 1600 million years ago (Ma)] (*12–14*).

Seismic velocities in the lithospheric mantle beneath the Kaapvaal-Zimbabwe craton were mapped using teleseismic broadband waveforms (*2*, *3*) (Fig. 1). The Kaapvaal-Zimbabwe craton is marked by relatively high P-wave velocity lithospheric mantle that occurs in two prominent but irregularly shaped lobes separated by a broad WNW-trending band of relatively lower velocity mantle. Southern African diamonds were stored in the mantle with these differences in seismic velocity (Table 1, Fig. 1) because current seismic structure correlates with the Archean to Proterozoic surface geology, which is much older than the kimberlite eruptions. Jwaneng, Letlhakane, Orapa, and Premier diamonds were hosted in slower lithospheric mantle with P-wave velocities below the average model velocity (−0.21 to −0.01%). De Beers Pool, Finsch, Jagersfontein, Koffiefontein, Roberts Victor, and Venetia diamonds were hosted in faster mantle with P-wave velocities above the average model velocity (+0.08 to +0.36%).

Harzburgitic (*15*) silicate inclusions in diamonds from the De Beers Pool and Finsch in the seismically fast lithosphere have mid-Archean model ages [3.2 to 3.3 billion year (Gy)] (*10*); all other silicate inclusions dated so far are lherzolitic or eclogitic and are Proterozoic in age (*11*, *16–18*) (Table 2). Eclogitic sulfide inclusions from both fast and slower lithosphere have late Archean (2.9 Gy) (*19–21*) and Proterozoic ages that match those of the eclogitic silicate inclusions.

Diamonds from kimberlites in seismically fast lithosphere are dominantly peridotitic (*15*), whereas diamonds from kimberlites in slower lithosphere are dominantly eclogitic (*22–30*) (Table 1, Fig. 1) (fig. S1). This relation holds for 9 of the 10 localities studied, with Jagersfontein, which has asthenospheric diamonds (*28*), as the exception. Both peridotitic and eclogitic diamonds have prevalent mantle-like carbon isotopic composition [$\delta^{13}C$ = −3 to −7 per mil (‰)], but eclogitic diamonds have an isotopically light subpopulation ($\delta^{13}C$ = −22 to −10‰) (Fig. 2A) (*31*, *32*). The diamonds from the slower lithospheric mantle have a greater frequency of isotopically light carbon, a higher percentage of type Ia diamonds (*33*), and a population with higher average N content (Figs. 2B and 3, A and B).

Two groups of diamond localities can be designated: those above fast mantle, whose diamonds are dominantly peridotitic with low N content [170 to 259 parts per million (ppm)], and those above slower mantle, whose diamonds are dominantly eclogitic with higher N content (345 to 478 ppm). The ecologitic diamonds incorporated more N during their growth. Whether this was due to a diamond-forming fluid with higher N or faster growth of these diamonds is not clear. Because these diamonds are at least Proterozoic, the correlation of diamond composition, inclusion paragenesis, and seismic velocity suggests that the seismic structure of the craton is a mid-Proterozoic overprint to an Archean keel, which has been frozen in since the mid-Proterozoic.

Seismic velocity is dependent on temperature, but a 1.2-billion-year-old cold cratonic geothermal gradient from Premier (*34*, *35*) (in the slow region) suggests composition may be more important. The slow region of the lithosphere (Fig. 1) may be higher in basaltic components (Fe, Ca, clinopyroxene) or metasomatizing fluids that hydrated and altered the host peridotite and could account for a 1% reduction in P-wave velocity (*36*). Premier peridotite xenoliths and diamonds provide the best exam-

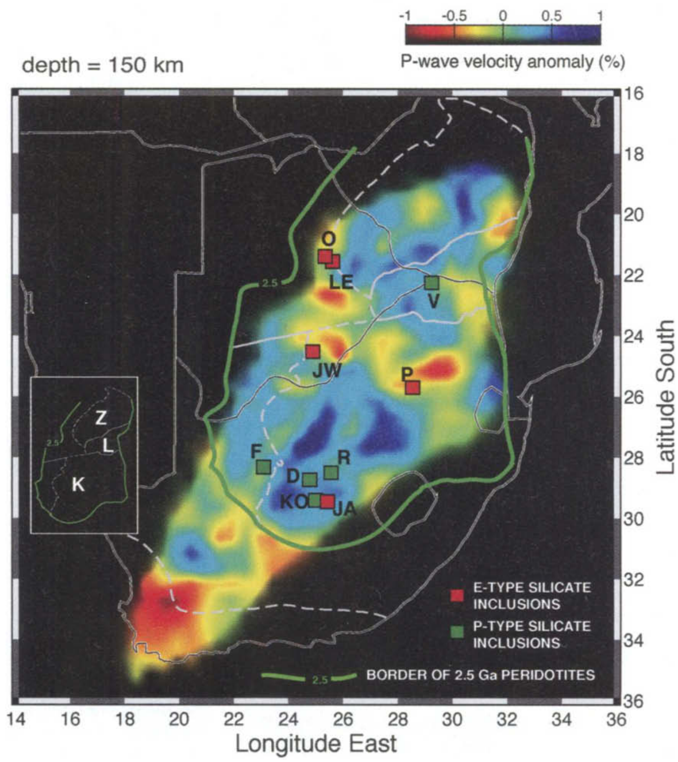

Fig. 1. Tomographic image of the lithospheric mantle in the diamond stability field (150 km depth) derived from seismic P-wave data (*2*, *3*). (Inset) The Kaapvaal (K) and Zimbabwe (Z) cratonic blocks and the Limpopo (L) mobile belt are referred to collectively in the text as the Kaapvaal-Zimbabwe craton. Bold green line indicates the outermost boundary of the Kaapvaal-Zimbabwe craton (*1*, *37*, *50*). Colored squares represent diamond mines as follows: red, predominantly eclogitic silicate inclusions (Jagersfontein, JA; Jwaneng, JW; Letlhakane, LE; Orapa, O; Premier, P), and green, predominantly peridotitic silicate inclusions (Kimberley area mines of Bultfontein, De Beers, Dutoitspan, and Wesselton termed De Beers Pool, D; Finsch, F; Koffiefontein, KO; Roberts Victor, R; and Venetia, V). See fig. S1 for a cross section.

Table 2. Silicate or sulfide inclusion age and paragenesis for diamonds from the major diamond mines of southern Africa. About 100 individual sulfide inclusions have been analyzed for Re-Os ages; about 3000 silicate inclusions (either composites or individual grains) have been analyzed for Sm-Nd ages. Sources of data are as follows: De Beers Pool (*10*, *20*), Finsch (*10*, *17*, *55*), Jwaneng (*18*, *56*), Koffiefontein (*19*), Orapa (*17*, *57*), and Premier (*11*, *16*).

Location	Sulfide inclusions		Silicate inclusions	
	Re-Os Age (Ma)	Paragenesis	Sm-Nd Age (Ma)	Paragenesis
Jwaneng	1500 to 2900	E	1540	E
Orapa	1000 to 2900	E	990	E
Premier			1150 to 1930	E,(P)
De Beers Pool	2900	E	3200	P
Finsch			1580 to 3200	P,(E)
Koffiefon	1000 to 2900	E		

[1]Department of Terrestrial Magnetism, Carnegie Institution of Washington, 5241 Broad Branch Road NW, Washington, DC 20015, USA. [2]Division of Earth Sciences, University of Glasgow, Glasgow G12 8QQ, UK. [3]Department of Geological Sciences, University of Cape Town, Rondebosch 7701, South Africa. [4]Department of Geological Sciences, Arizona State University, Post Office Box 871404, Tempe, AZ 85287–1404, USA. [5]Laboratoire de Geochimie des Isotopes Stables, Universite de Paris VII, Institut de Physique du Globe de Paris (IPGP), 4 Place Jussieu, 75251 Paris Cedex 05, France. [6]Department of Mineral Sciences, The Pennsylvania State University, University Park, PA 16802, USA. [7]De Beers GeoScience Centre, Post Office Box 82232, Southdale, 2135, South Africa.

*To whom correspondence should be addressed. E-mail: shirey@dtm.ciw.edu

ple of the former. Some xenoliths have Archean Re-Os model ages, whereas others have Re-Os systematics that are Proterozoic (*37*, *38*). The precursors of Premier peridotitic silicate inclusions in diamonds (lherzolitic garnet and clinopyroxene) that equilibrated at 1.9 Ga (*11*) have Archean mantle model ages.

All indications are that diamond formation in the cratonic mantle is episodic rather than continuous. The occurrence of 3.2- to 3.3-Ga diamonds with depleted harzburgitic silicate inclusions (*10*) and of 2.9-Ga diamonds with enriched eclogitic sulfide inclusions (*20*) in the De Beers Pool kimberlites (fig. S1) indicates that creation and assembly of the craton was at least a two-stage process. Isotopic ages suggest a time gap of 300 ± 200 million years between the two Archean diamond formation events. Cratonic nuclei were first created by mantle melting processes that produced severe depletion of peridotite and high-degree melts such as komatiites (*10*, *39*). Such depletion is now thought to have occurred at shallow depths (*40–42*), perhaps in a subduction zone setting (*43*), although previous suggestions have included mantle plumes (*44*, *45*). Oceanic lithosphere was then accreted to these early cratonic nuclei and contributed to the stabilization of the lithospheric mantle as indicated by the occurrence of 2.9-Ga eclogitic diamonds with a subduction signature (*20*), corresponding diamondiferous eclogites (*21*), the typical Re-Os model age for mantle peridotite (*37*, *38*), and evidence for continental collision in the crust from 2.88 to 2.94 Ga (*46*).

Compositional changes to the lithosphere and the formation of Proterozoic eclogitic diamonds are linked by their preferential occurrence in seismically slow lithosphere (Fig. 1) (fig. S1). The lherzolitic and eclogitic composition of Premier diamonds and the Proterozoic Re-Os model ages in Premier peridotite xenoliths attributable to interaction with melts of Bushveld age (2 Ga) (*37*, *38*) link diamond formation in the WNW-trending belt of slower lithospheric mantle to magmatism of the Bushveld–Molopo Farms complex. Along the western Kaapvaal-Zimbabwe craton margin, diamond formation may also be linked to crustal fluids carried to diamond source depths by subduction, as indicated by the eclogitic inclusion compositions, the lighter and more variable $\delta^{18}O$ of Jwaneng zircon megacrysts (*47*), and the light C and heavy N isotopic composition of Orapa diamonds (*48*). Available C and N isotope data for Orapa and Jwaneng diamonds require either mixing of mantle and crustal endmembers with variable C/N ratio or, alternatively, C and N isotopic fractionation during diamond formation (*23*, *48*, *49*). Either way, the history of creation, assembly, and modification of the Kaapvaal-Zimbabwe craton is reflected in the age and chemistry of the multiple generations of diamonds formed and stored in its lithospheric mantle keel.

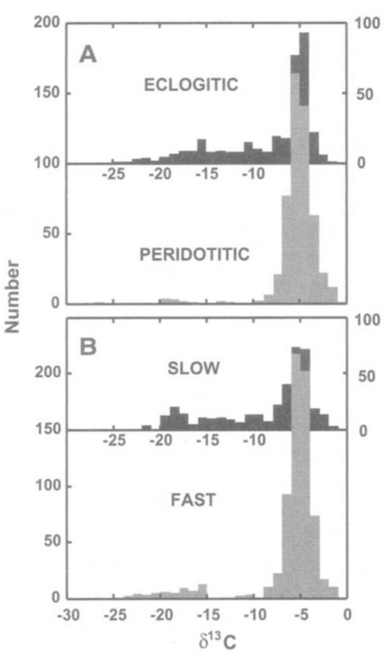

Fig. 2. (**A**) Comparison of the carbon isotopic composition of individual diamond analyses grouped according to their paragenesis. Both eclogitic and peridotitic histograms include diamonds from all nine localities. (**B**) Comparison of the carbon isotopic composition of southern African diamonds, grouped according to their derivation from a locality in seismically or fast lithospheric mantle. Sources of data are given in Table 1.

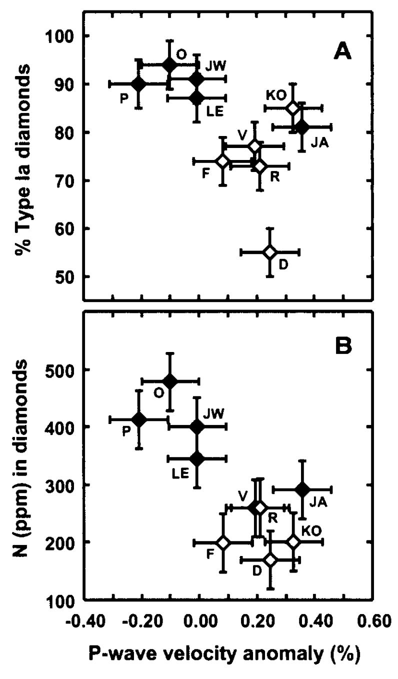

Fig. 3. Percentage of type Ia diamonds (**A**) and average N abundance in diamonds (**B**) versus P-wave velocity anomaly. Error bars have been set at the ±5% level for percentage of type Ia diamonds, ±50 ppm for average N abundance, and ±0.1% for P-wave velocity anomaly. Letters represent diamond mines as defined in Fig. 1. Peridotitic, open symbols; eclogitic, closed symbols.

References and Notes

1. R. W. Carlson, T. L. Grove, M. J. de Wit, J. J. Gurney, *Eos* **77**, 273 (1996).
2. D. E. James, M. J. Fouch, in *Early Earth*, C. Ebinger, M. Fowler, C. J. Hawkesworth, Eds. (Geological Society of London, in press).
3. D. E. James, M. J. Fouch, J. C. VanDecar, S. van der Lee, K. S. Group, *Geophys. Res. Lett.* **28**, 2485 (2001).
4. R. W. Carlson *et al.*, *GSA Today* **10**, 1 (2000).
5. J. W. Harris, in *The Properties of Natural and Synthetic Diamond*, J. E. Field, Ed. (Academic Press, New York, 1992), pp. 345–393.
6. D. G. Pearson, S. B. Shirey, in *Application of Radiogenic Isotopes to Ore Deposit Research and Exploration*, D. D. Lambert, J. Ruiz, Eds. (Society of Economic Geologists, Denver, CO, 1999), vol. 12, pp. 143–172.
7. F. R. Boyd, J. J. Gurney, *Science* **232**, 472 (1986).
8. A. J. A. Janse, *Russ. Geol. Geophys.* **33**, 9 (1992).
9. The Archean Eon extends from 3.8 Ga to 2.5 Ga. The Proterozoic Eon extends from 2.5 Ga to 544 Ma.
10. S. H. Richardson, J. J. Gurney, A. J. Erlank, J. W. Harris, *Nature* **310**, 198 (1984).
11. S. H. Richardson, J. W. Harris, J. J. Gurney, *Nature* **366**, 256 (1993).
12. G. L. Davis, T. E. Krogh, A. J. Erlank, *Carnegie Inst. Washington Year Book* **75**, 821 (1976).
13. G. L. Davis, *Carnegie Inst. of Washington Year Book* **76**, 631 (1977).
14. C. B. Smith, H. L. Allsopp, J. D. Kramers, G. Hutchinson, J. C. Roddick, *Trans. Geol. Soc. S. Africa* **88**, 249 (1985).
15. Harzburgitic diamonds have low Ca and high Cr garnet inclusions named after harzburgite, a depleted mantle rock. Lherzolitic diamonds have higher Ca and lower Cr content garnet and clinopyroxene inclusions named after lherzolite, a less depleted mantle rock. Both diamond types are called "P-type" after peridotite, the general name for harzburgite and lherzolite. Other P-type diamonds contain Fe-sulfide inclusions that are high in Ni. Eclogitic diamonds ("E-type") have pyrope-almandine garnet, omphacitic clinopyroxene, or Fe-sulfide inclusions with low Ni content characteristic of eclogite, a high-pressure metamorphosed basalt.
16. S. H. Richardson, *Nature* **322**, 623 (1986).
17. ______, A. J. Erlank, J. W. Harris, S. R. Hart, *Nature* **346**, 54 (1990).
18. S. H. Richardson, I. L. Chinn, J. W. Harris, in *The P. H. Nixon Volume*, J. J. Gurney, J. L. Gurney, M. D. Pascoe, S. H. Richardson, Eds. (Red Roof Design, Cape Town, 1999), pp. 734–736.
19. D. G. Pearson, S. B. Shirey, J. W. Harris, R. W. Carlson, *Earth Planet. Sci. Lett.* **160**, 311 (1998).
20. S. H. Richardson, S. B. Shirey, J. W. Harris, R. W. Carlson, *Earth Planet. Sci. Lett.* **191**, 239 (2001).
21. S. B. Shirey *et al.*, *Geophys. Res. Lett.* **28**, 2509 (2001).
22. P. Cartigny, thesis, Universite de Paris VII (1998).
23. ______, J. W. Harris, M. Javoy, *Science* **280**, 1421 (1998).
24. P. Deines, J. W. Harris, J. J. Gurney, *Geochim. Cosmochim. Acta* **57**, 2781 (1993).
25. P. Deines, J. J. Gurney, J. W. Harris, *Geochim. Cosmochim. Acta* **48**, 325 (1984).
26. P. Deines, J. W. Harris, *Geochim. Cosmochim. Acta* **59**, 3173 (1995).
27. ______, J. J. Gurney, *Geochim. Cosmochim. Acta* **51**, 1227 (1987).
28. ______, *Geochim. Cosmochim. Acta* **55**, 2615 (1991).
29. P. Deines, J. W. Harris, P. M. Spear, J. J. Gurney, *Geochim. Cosmochim. Acta* **53**, 1367 (1989).
30. P. Deines, J. W. Harris, J. J. Gurney, *Geochim. et Cosmochim. Acta* **61**, 3993 (1997).
31. J. J. Gurney, in *Kimberlites and Related Rocks*, J. Ross *et al.*, Eds. (Geological Society of Australia, Sydney, Australia, 1989), vol. 14, pp. 935–965.

32. M. B. Kirkley, J. J. Gurney, A. A. Levinson, *Gems Gemol.* **27**, 2 (1991).
33. Diamonds with no or low (<20 ppm) N are termed Type II. Diamonds with spectroscopically detectable N (termed Type Ia, Table 1) show a N distribution that progresses from C-centers (single N) through A-centers (paired N) to B-centers (clusters of four N and a vacancy) in proportion with geological time (hundreds of Ma), temperature, and nitrogen content. Of these three variables, N aggregation will be sensitive chiefly to temperature. See (*49*) for details.
34. R. V. Danchin, in *The Mantle Sample: Inclusions in Kimberlites and Other Volcanics*, F. R. Boyd, H. O. A. Meyer, Eds. (American Geophysical Union, Washington, DC, 1979), vol. 2, pp. 104–126.
35. M. Q. W. Jones, *J. Geophys. Res.* **93**, 3243 (1988).
36. T. H. Jordan, in *The Mantle Sample; Inclusions in Kimberlites and Other Volcanics*, F. R. Boyd, H. O. A. Meyer, Eds. (American Geophysical Union, Washington, DC, 1979), vol. 2, pp. 1–14.
37. R. W. Carlson *et al.*, in *The J. B. Dawson Volume*, J. J. Gurney, J. L. Gurney, M. D. Pascoe, S. H. Richardson, Eds. (Red Roof Design, Cape Town, 1999), pp. 99–108.
38. G. J. Irvine, D. G. Pearson, R. W. Carlson, *Geophys. Res. Lett.* **28**, 2505 (2001).
39. R. J. Walker, R. W. Carlson, S. B. Shirey, F. R. Boyd, *Geochim. Cosmochim. Acta* **53**, 1583 (1989).
40. D. Canil, K. Wei, *Contrib. Mineral. Petrol.* **109**, 421 (1992).
41. T. Stachel, K. S. Viljoen, G. Brey, J. W. Harris, *Earth Planet. Sci. Lett.* **159**, 1 (1998).
42. M. J. Walter, *J. Petrol.* **39**, 29 (1998).
43. S. W. Parman, J. C. Dann, T. L. Grove, *Geophys. Res. Lett.* **28**, 2513 (2001).
44. S. E. Haggerty, *Nature* **320**, 34 (1986).
45. N. T. Arndt, A. C. Kerr, J. Tarney, *Earth Planet. Sci. Lett.* **146**, 289 (1997).
46. M. D. Schmitz, thesis, Massachusetts Institute of Technology (2002).
47. J. W. Valley, P. D. Kinny, D. J. Schulze, M. J. Spicuzza, *Contrib. Mineral. Petrol.* **133**, 1 (1998).
48. P. Cartigny, J. W. Harris, M. Javoy, *Earth Planet. Sci. Lett.* **185**, 85 (2001).
49. O. Navon, in *The P.H. Nixon Volume*, J. J. Gurney, J. L. Gurney, M. D. Pascoe, S. H. Richardson, Eds. (Red Roof Design, Cape Town, 1999), pp. 584–604.
50. P. E. Janney, R. W. Carlson, S. B. Shirey, D. R. Bell, A. P. le Roex, paper presented at the Ninth Annual V. M. Goldschmidt Conference, Cambridge, MA, 22 to 26 August 1999.
51. J. W. Harris, unpublished data.
52. P. Deines, J. W. Harris, D. N. Robinson, J. J. Gurney, S. R. Shee, *Geochim. Cosmochim. Acta* **55**, 515 (1991).
53. H. J. Milledge *et al.*, *Nature* **303**, 791 (1983).
54. P. Deines, F. Viljoen, J. W. Harris, *Geochim. Cosmochim. Acta* **65**, 813 (2001).
55. C. B. Smith *et al.*, *Geochim. Cosmochim. Acta* **55**, 2579 (1991).
56. S. H. Richardson, unpublished data.
57. S. Shirey *et al.*, unpublished data.
58. Discussions with D. Bell, R. Carlson, I. Chinn, D. G. Pearson, and K. Westerlund are greatly appreciated, as is the assistance of T. Mock and M. Horan in the DTM mass spectrometry and chemistry labs, respectively. We appreciate V. Anderson, E. van Blerk, R. Ferraris, R. Hamman, W. Moore, A. Ntidisang, G. Parker, and others at Harry Oppenheimer House, Kimberley, for their skill in selecting specimens, and we thank the De Beers Diamond Trading Company for making them available. The manuscript was improved by the reviews of F. Boyd, K. Burke, R. Carlson, E. Hauri, T. Stachel, and E. Vicenzi. Support was chiefly from NSF EAR Continental Dynamics Grant 9526840.

Supporting Online Material
www.sciencemag.org/cgi/content/full/297/5586/1683/DC1
Fig. S1

29 March 2002; accepted 29 July 2002

Identification of a DNA Nonhomologous End-Joining Complex in Bacteria

Geoffrey R. Weller,[1]* Boris Kysela,[2]* Rajat Roy,[3]* Louise M. Tonkin,[1] Elizabeth Scanlan,[4] Marina Della,[1] Susanne Krogh Devine,[4] Jonathan P. Day,[5] Adam Wilkinson,[5] Fabrizio d'Adda di Fagagna,[3] Kevin M. Devine,[4] Richard P. Bowater,[5] Penny A. Jeggo,[2] Stephen P. Jackson,[3] Aidan J. Doherty[1]†

In eukaryotic cells, double-strand breaks (DSBs) in DNA are generally repaired by the pathway of homologous recombination or by DNA nonhomologous end joining (NHEJ). Both pathways have been highly conserved throughout eukaryotic evolution, but no equivalent NHEJ system has been identified in prokaryotes. The NHEJ pathway requires a DNA end-binding component called Ku. We have identified bacterial Ku homologs and show that these proteins retain the biochemical characteristics of the eukaryotic Ku heterodimer. Furthermore, we show that bacterial Ku specifically recruits DNA ligase to DNA ends and stimulates DNA ligation. Loss of these proteins leads to hypersensitivity to ionizing radiation in *Bacillus subtilis*. These data provide evidence that many bacteria possess a DNA DSB repair apparatus that shares many features with the NHEJ system of eukarya and suggest that this DNA repair pathway arose before the prokaryotic and eukaryotic lineages diverged.

Double-strand breaks (DSBs) in DNA arise during exposure to ionizing radiation (IR) and as intermediates during site-specific rearrangement events such as mating-type switching in *Saccharomyces cerevisiae* and V(D)J recombination in vertebrates (*1*, *2*). In eukaryotic cells, the primary DNA end-binding component of NHEJ, Ku, is a heterodimer of two sequence-related subunits [Ku70 (69 kD) and Ku80 (83 kD)] (*3–5*) that forms an open ringlike structure through which a variety of DNA end structures can be threaded (*6*, *7*). DNA-bound Ku helps to recruit the ligase IV/XRCC4 complex, thereby enhancing its ligation activity (*8–10*). In vertebrates, Ku also recruits the DNA-dependent protein kinase catalytic subunit (DNA-PKcs), thereby activating its kinase activity, which is required for DSB rejoining (*11–13*). Mammalian cells deficient in these NHEJ proteins are defective in DSB rejoining and are hypersensitive to IR (*1*, *4*, *13*).

In contrast to the conservation between these components in higher and lower eukaryotes, NHEJ has not been reported in prokaryotes. However, genes with significant homology to Ku70 and Ku80 have been identified in some bacterial genomes (*14*, *15*), which raises the possibility that prokaryotes might have a NHEJ apparatus that is fundamentally homologous to that of eukaryotic cells. Significantly, the Ku-like gene exists in some bacterial species in an operon that includes a gene predicted to encode an adenosine triphosphate (ATP)–dependent DNA ligase (*14–16*). Operons frequently co-regulate functionally interacting proteins (*17*); perhaps then, these putative ligases interact with the Ku-like proteins.

We exploited the genetically amenable bacterium *Bacillus subtilis* to generate strains bearing inactivating mutations in *YkoV* (Ku-like gene; *ykoV*) and *YkoU* (ligase-like gene; *ykoU*) and double mutants defective in *YkoU* and *YkoV* (ykoU ykoV) (*18*). None of the strains had any observable growth defect at temperatures ranging from 10° to 37°C (*19*), which indicates that neither *YkoU* nor *YkoV* is essential. These findings are consistent with the notion that the *B. subtilis* nicotinamide adenine dinucleotide (NAD^+)–dependent ligase *YerG* functions during DNA replication (*20*). To investigate the role of *YkoU* and *YkoV* in DNA repair, we examined the sensitivity of the mutant strains to DNA-damaging agents (*18*). No sensitivity to ultraviolet light or to methyl methanesulfonate (MMS) was observed, which suggests that nucleotide excision repair functions normally and alkylation damage induced by MMS is repaired efficiently (*19*). In contrast,

[1]Cambridge Institute for Medical Research & Department of Haematology, University of Cambridge, Hills Road, Cambridge CB2 2XY, UK. [2]Genome Damage and Stability Centre, University of Sussex, Brighton BN1 9RQ, UK. [3]Wellcome Trust/Cancer Research UK, Institute of Cancer and Developmental Biology and Department of Zoology, University of Cambridge, Tennis Court Road, Cambridge, CB2 1QR, UK. [4]Department of Genetics, Smurfit Institute, Trinity College Dublin, Dublin 2, Republic of Ireland. [5]School of Biological Sciences, University of East Anglia, Norwich NR4 7TJ, UK.

*These authors contributed equally to this work.
†To whom correspondence should be addressed. E-mail: AJD42@cam.ac.uk.